Electronic Supplementary Material (ESI) for Physical Chemistry Chemical Physics.

Supporting Information

Molecular Torsion Controls the Excited State Relaxation Pathways of Multibranched Tetraphenylpyrazines: Effect of Substitution of Morpholine Vs Phenoxazine

Hasim Fayiz Pananilath[a,b], Chinju Govind[a,b], Tessy D. Thadathilanickal[a,b], Venugopal Karunakaran[a,b *]

[a]Photosciences and Photonics Section, Chemical Sciences and Technology Division, CSIR-National Institute for Interdisciplinary Science and Technology, Thiruvananthapuram-695 019, Kerala, India, [b]Academy of Scientific and Innovative Research (AcSIR), Ghaziabad, 201002, India.

*E–mail: k.venugopal@niist.res.in; Phone: 091–471–2515240.

Table of content **Page No.**

1. Experimental Section

1.1 General details: The reagents and materials were purchased from Sigma–Aldrich and TCI. ^{1}H and ^{13}C NMR spectra were recorded using a Bruker AMX spectrometer at 500 and 125 MHz respectively using tetramethylsilane (TMS) as an internal standard. High resolution mass spectra were recorded using Thermo Scientific Exactive–LCMS by electron spray ionization method. The matrix assisted laser desorption ionization time–of–flight (MALDI–TOF) mass spectra were recorded using Bruker Autoflex speed instrument.

1.2 Steady state measurements: Steady state absorption spectra and fluorescence spectra were recorded using UV–Visible absorption spectrophotometer (Shimadzu, UV–2600) and a fluorescence spectrometer (FluoroLog–3, Horiba, equipped with a 450 W Xenon arc lamp) at ambient temperature, respectively. The fluorescence quantum yields of compounds were determined in various solvents by the relative method employing quinine sulphate as a reference (Φ_R = 0.54) by adjusting same absorbance at the excitation wavelength. The following equation was used for calculating relative fluorescence quantum yield

$$\Phi_S = \frac{Abs_R}{Abs_S} \times \frac{Area_S}{Area_R} \times \frac{\eta_S^2}{\eta_R^2} \times \Phi_R \quad (1)$$

where subscripts R and S refer to the reference and sample, respectively. Abs, Area and η are the absorbance at the excitation wavelength, area under the fluorescence spectrum and refractive index of the solvent, respectively.

1.3 Electrochemical measurements: Electrochemical measurements were carried in N_2-purged dichloromethane by using CHI-660 voltametric analyzer with three electrode cell assemblies. Tetrabutylammonium hexafluorophosphate, N-Bu_4PF_6, was used as the supporting electrolyte. The conventional three-electrode configuration consists of a platinum wire as a counter electrode, glassy carbon as a working electrode and $Ag/AgNO_3$ couple as a reference

electrode. The ferrocenium/ ferrocene (Fc^+/Fc) redox couple was used as the internal standard. Cyclic voltammograms were obtained at a scan rate of 100 mV s^{-1}.

1.4 DLS Measurements: Dynamic light scattering (DLS) experiments were performed on Malvern Instrument's Zetasizer Nano Series (Zeta Nano-ZS). The size distribution of the aggregates was measured in a 10 mm quartz cuvette with a final volume of 1 mL, at 20 °C, in three consecutive runs of the same. The refractive index of water is used for analysis of particle size in f_w = 90%.

1.5 Theoretical calculations: Theoretical calculations were carried out using Density Functional Theory (DFT) with the CAM-B3LYP functional and the 6-31G (d) basis set. The ground state geometry was optimized using Gaussian 09.[1] The same optimized ground state geometry was used to calculate S_1 and T_1 vertical excitation energy.

1.6 Time correlated single photon counting (TCSPC): Fluorescence lifetimes were measured by using a picosecond single photon counting system (Horiba, DeltaFlex). The samples were excited by employing 378 nm LED as excitation sources and detected using picosecond photon detection module (PPD-850). The fluorescence time constants are obtained by deconvoluting with the LED profiles. The decay of the fluorescence intensity (I) with time (t) was fitted either by a mono or double-exponential function

$$I = A_1 e^{-\frac{t}{\tau_1}} \quad (2)$$

$$I = A_1 e^{-\frac{t}{\tau_1}} + A_2 e^{-\frac{t}{\tau_2}} \quad (3)$$

where t_1 and t_2 are the lifetimes of different species, and A_1 and A_2 are their respective amplitudes.

1.7 Nanosecond transient absorption spectra: Nanosecond transient absorption spectra were obtained by exciting the samples with the third harmonic of fundamental light (1064 nm) from an Quanta Ray Nd: YAG laser (wavelength, 355 nm, ~10 ns) and using an Applied Photophysics model LKS 60 laser kinetics spectrometer. The probing light source was a 150 W Xenon arc lamp. The light of the probe transmitted through a 1 cm quartz cuvette was dispersed by a monochromator and detected by a photomultiplier tube coupled to a digital oscilloscope (Agilent Infiniium DSO8064A, 600 MHz, 4 $GSas^{-1}$). The analyzing and laser beams were fixed at right angles to each other. The power of each laser pulse was monitored using a fast silicon photodiode.

Quantification of triplet state properties of TPP derivatives

In order to measure the triplet quantum yields of TPP derivatives using $Ru(bpy)_3^{2+}$, we measured the energy transfer to β carotene with a previously described method.[2] This experiment used optically matched $Ru(bpy)_3^{2+}$ and TPP derivatives mixed with a β carotene of known concentration. The transient absorbance (ΔA) of the β carotene triplet, formed by the energy transfer from $Ru(bpy)_3^{2+}$ or the TPP derivatives triplet, was monitored at 520 nm. Comparison of plateau absorbance following the completion of sensitized triplet formation, properly corrected for the decay of the donor triplets in competition with energy transfer to β carotene, enabled us to estimate Φ_T of TPP derivatives based on equation.[2]

$$\Phi_T{}^S = \Phi_T{}^R \frac{\Delta A^S}{\Delta A^R} \frac{k_{obs}^S}{k_{obs}^S - k_0^S} \frac{k_{obs}^R - k_0^R}{k_{obs}^R} \quad (4)$$

where superscripts 'S' and 'R' designate the different TPP derivatives and $Ru(bpy)_3^{2+}$, respectively, k_{obs}, is the pseudo-first-order rate constant for the growth of the β carotene triplet and k_0 is the rate constant for the decay of the donor triplets, in the absence of β carotene observed in solutions containing $Ru(bpy)_3^{2+}$ or TPP derivatives at the same optical density

(OD) as those used for sensitization. As a result of negligible triplet yield, direct excitation of β carotene did not result in any significant triplet formation under these conditions. For $Ru(bpy)_3^{2}$+ in methanol, the triplet quantum yield was assumed to be one. This method yields reliable data and is consistent with the assumption that energy transfer to β carotene is 100% efficient.

1.8 Femtosecond transient absorption measurements: The seed laser is the Ti:sapphire laser (MaiTai HP, Spectra Physics, USA) having a center wavelength of 800 nm with a pulse width of <100 fs and a repetition rate of 80 MHz. The amplified laser was divided into two and the beam with high energy was used for exciting the compounds (385 nm) using TOPAS (prime, light conversion). The other portion (200 mW) of the amplified beam was focused on a CaF_2 plate (1 mm) to obtain a white light continuum (340− 1000 nm) that further divided into two beams (reference and sample probe beams). The sample (0.4 mm thickness) was refreshed by spinning at a constant speed. After passing through the sample, the white light continuum was focused into an optical fiber (100 μm) attached to the imaging spectrometer. The spectrophotometer setup is ExciPro, CDP Systems Corp, Russia. The transient absorption spectra were recorded at a magic angle (54.7°) by averaging about 2000 excitation pulses for each delay time. All the transient absorption spectra are corrected for chirp of the white light by estimating the time zero with the coherent artifact found in the solvent. The laser fluence used for all the transient absorption measurements is ~3 $\mu J/cm^2$. The IRF of the ultrafast spectrometer is found to be about ≤120 fs. The stability of the sample is checked by recording the absorption spectra of the sample (before and after the measurements) and observed to have no substantial differences in the absorption spectra. The absorbance of solutions of TPP derivatives was ~0.7 OD for femtosecond transient absorption measurements.

2. Synthesis and characterisation details of TPP derivatives:

Synthesis of 1,2-bis(4-bromophenyl)-2-hydroxyethanone (2): Thiamine hydrochloride (2.0 mmol) was dissolved in 1mL of water in a 100 mL round bottom flask followed by adding 6.5 mL of EtOH and the solution was cooled down to 0°C and the mixture of solution was stirred well. The pH of solution (9-10) was adjusted by adding 8% cold NaOH aqueous solution. Then, 4-bromo benzaldehyde **1** (8 mmol) was added very slowly to the above mixture. The solution mixture was heated at 60°C for 12 h. The reaction mixture was extracted using dichloromethane solvent. The organic layer was washed thoroughly with water and dried over anhydrous sodium sulphate. The excess solvent was removed under reduced pressure and the crude product was further purified by column chromatography using silica (100-200 mesh) as the stationary phase and EtOAc/Hexane mixture (10:90) as the eluting solvent. Yield 28%; White solid. ^{1}H NMR (500 MHz, $CDCl_3$): δ 7.75-7.73 (d, 2H), 7.56-7.55 (d, 2H), 7.47-7.45 (d, 2H), 7.19-7.18 (d, 2H), 5.86-5.85 (d, 1H), 4.49-4.48 (d, 1H) ppm; ^{13}C NMR (125 MHz, $CDCl_3$): δ 197.63, 137.61, 132.42, 132.21, 131.93, 130.47, 129.56, 129.36, 122.99, 75.53 ppm.

Synthesis of 2,3,5,6-tetrakis(4-bromophenyl)pyrazine (3): The mixture of 1,2-bis(4-bromophenyl)-2-hydroxyethanone (1.35 mmol) and NH_4OAc (6.4 mmol), $CeCl_3.7H_2O$ (0.13 mmol) and ethanol (6 ml) were kept over 4 h under refluxing condition . The mixture was cooled down to room temperature. The reaction mixture was then extracted with dichloromethane. The organic layer was washed thoroughly with water and dried over anhydrous sodium sulphate. The excess solvent was removed under reduced pressure and the crude product was further purified by column chromatography using silica gel (100-200 mesh) as the stationary phase and EtOAc/Hexane mixture (5:95) as the eluting solvent. Yield: 48%; White solid. ^{1}H NMR (500 MHz, $CDCl_3$): δ 7.48 (s,16H) ppm; ^{13}C NMR (125 MHz, $CDCl_3$):

δ 147.39, 136.68, 131.75, 131.33, 123.69 ppm; HRMS: (ESI+): m/z calcd for $C_{28}H_{16}{}^{81}Br_3{}^{79}BrN_2H_{17}$: 700.8047[M]$^+$; found: 700.8094.

TPP-4MOP: The compound was synthesized by using solvent free Buchwald- Hartwig reaction according the reported procedure.[3] The intermediate **3** (1.05 mmol), morpholine (4.2 mmol), palladium acetate (0.04 mmol), 2-dicyclohexylphosphino-2′,6′-diisopropoxybiphenyl (RuPhos, 0.08 mmol), and powdered sodium tert-butoxide (4.4 mmol) were added in to a screw cap vial. The reaction vial was transferred to a preheated oil bath (110 °C). After 24 h, the reaction mixture was cooled and dissolved in CH_2Cl_2/H_2O mixture (1:1). The organic phase was separated, the solvent was evaporated and the product was isolated by chromatography using a silica gel (100-200 mesh) as the stationary phase and 2% Methanol: CH_2Cl_2 as the mobile phase. The compound is further purified with HPLC chromatography. Yield, 65%; Yellow solid.^{1}H NMR (500 MHz, $CDCl_3$): δ 7.62-7.61 (d, 8H), 6.85-6.83 (d, 8H), 3.87-3.85 (t, 16H), 3.21-3.19 (t, 16H) ppm; ^{13}C NMR (125 MHz, $CDCl_3$): δ 151.02, 146.26, 130.68, 130.31, 114.77, 66.85, 48.75 ppm; HRMS (ESI+): m/z calcd for $C_{44}H_{48}N_6O_4$: 724.3737 [M+H]$^+$; found: 725.3816.

TPP-4PHO: The intermediate **3** (1.4 mmol), phenoxazine (7 mmol), palladium acetate (0.05 mmol), mmol), tri(tert-butyl)phosphine (0.11 mmol) and potassium carbonate (4.2 mmol) were dissolved in dry toluene (40 ml) and refluxed at 120°C for 24 h under argon atmosphere. On completion of the reaction, the reaction mixture was cooled to room temperature and dissolved in CH_2Cl_2/H_2O mixture (1:1). The organic phase was separated and the solvent was removed under reduced pressure. The product was purified by column chromatography using a silica gel (100-200 mesh) as the stationary phase and 2% Methanol: CH_2Cl_2 as the eluting solvent. Yield, 69%; Yellow solid. ^{1}H NMR (500 MHz, $CDCl_3$): δ 7.94-7.92 (d, 8H), 7.41-7.39 (d, 8H), 6.71-6.69 (d, 8H), 6.66-6.63 (t, 8H), 6.57-6.54 (t, 8H), 6.00-5.98 (d, 8H) ppm; ^{13}C NMR (125 MHz,

$CDCl_3$): δ 147.69, 142.95, 138.86, 137.06, 132.94, 131.59, 129.92, 122.36, 120.60, 114.59, 112.12 ppm; MALDI-TOF: m/z calcd for $C_{76}H_{48}N_6O_4$: 1108.3737 $[M+H]^+$; found: 1109.3817.

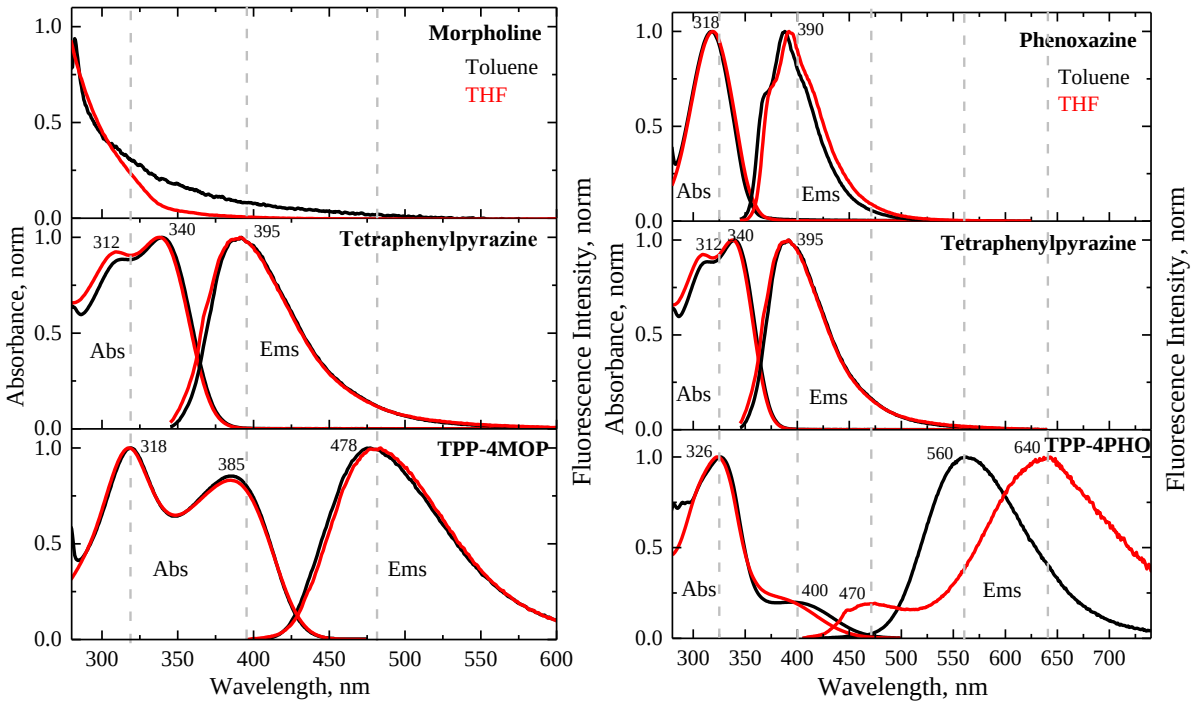

Figure S1 The absorption and emission spectra of individual chromophores of morpholine, phenoxazine and tetraphenylpyrazine (TPP) and also **TPP-4MOP** and **TPP-4PHO** in toluene (black) and THF (red). The morpholine did not show any emission.

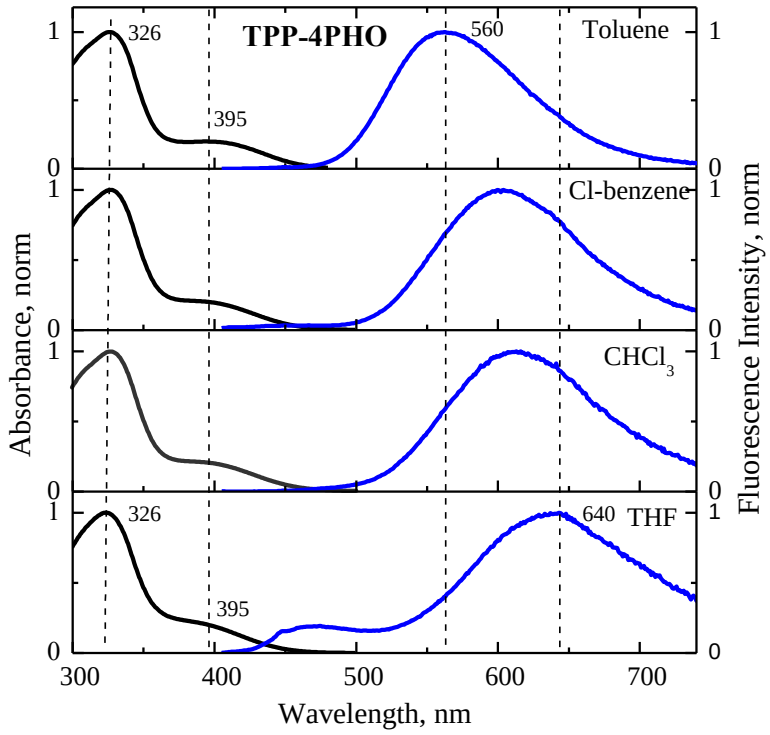

Figure S2 Absorption and emission spectra of **TPP-4PHO** in solvents of various polarities at room temperature.

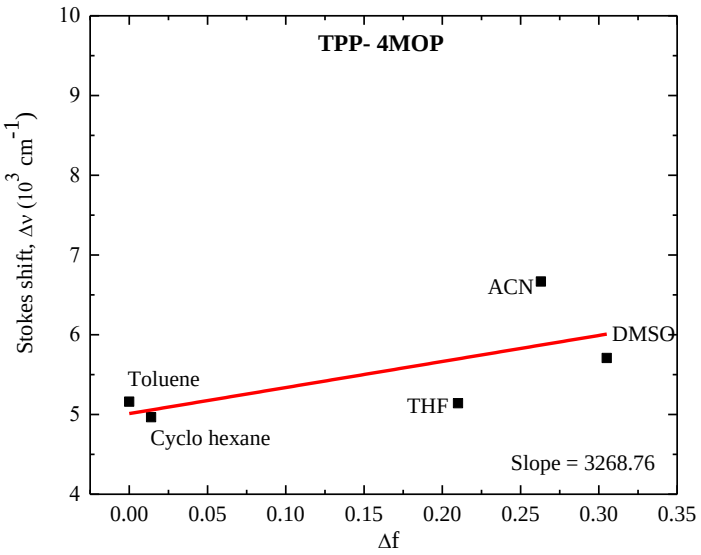

Figure S3 Lippert- Mataga plot of **TPP-4MOP**.

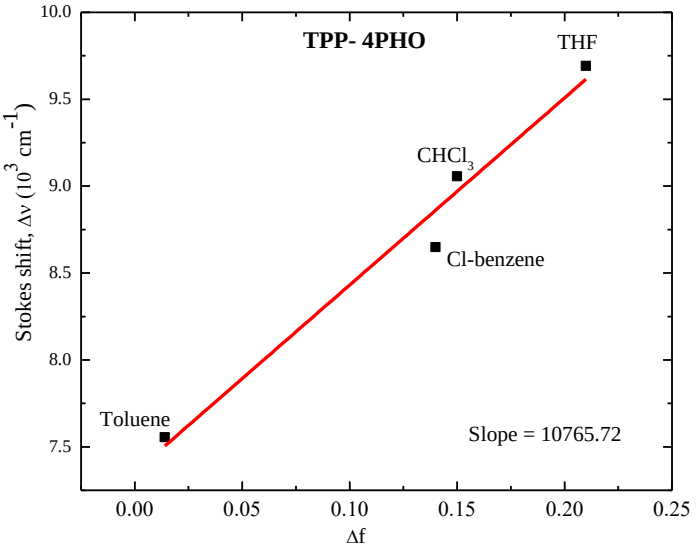

Figure S4 Lippert- Mataga plot of **TPP-4PHO**.

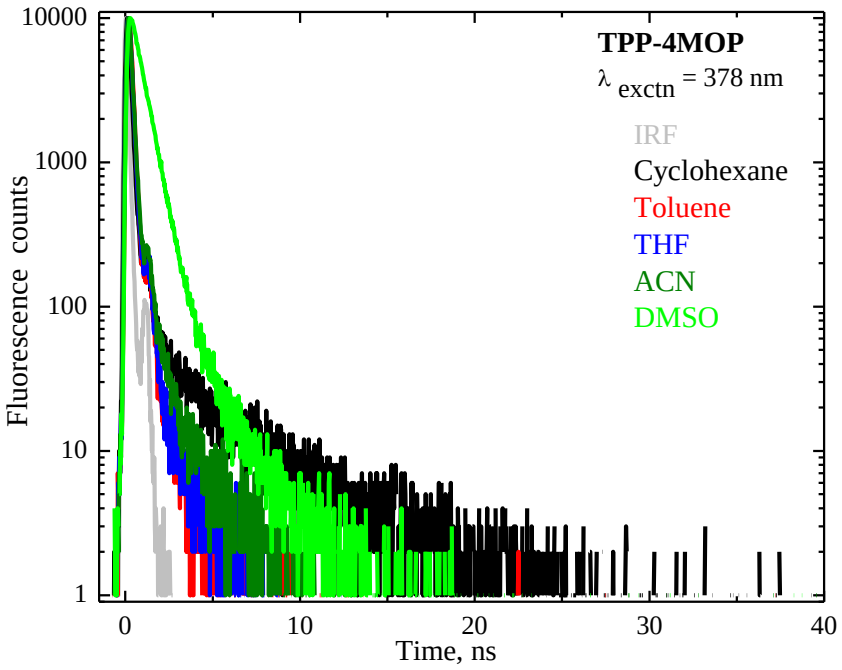

Figure S5 Fluorescence decay profile of **TPP-4MOP** in different solvents

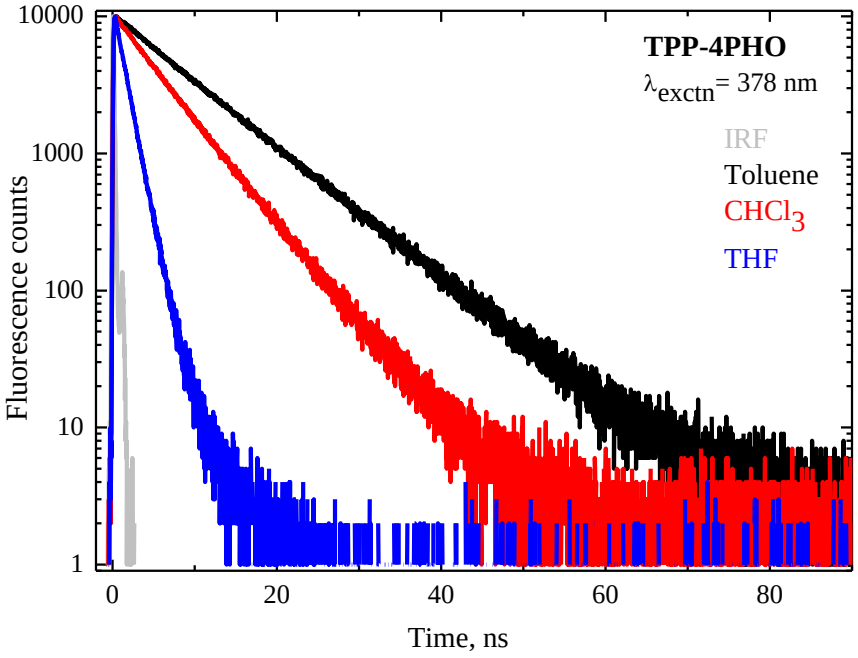

Figure S6 Fluorescence decay profile of **TPP-4PHO** in different solvents.

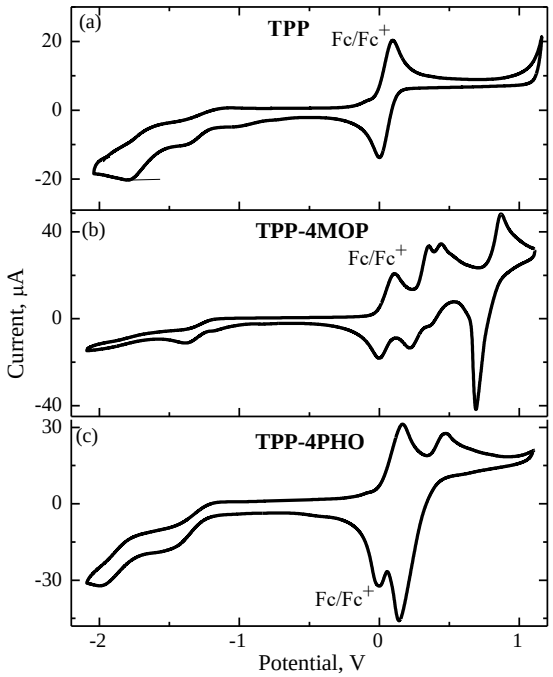

Figure S7 Cyclic voltammogram of **TPP** (a), **TPP-4MOP** (b) and **TPP-4PHO** (c) in dichloromethane. The internal standard, ferrocene (Fc) was used to set 0 V in the cyclic voltammograms. (Scan rate = 0.50 mV/s).

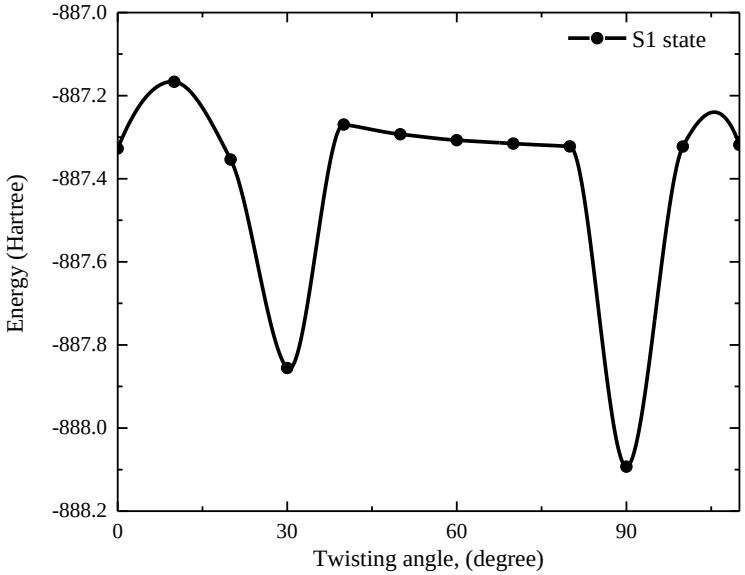

Figure S8 Theoretical potential energy surface (PES) diagram of **TPP-4PHO** in gaseous state for S_1 state calculated using TDDFT method, representing the changes in potential along the twisting angles of the phenoxazine group.

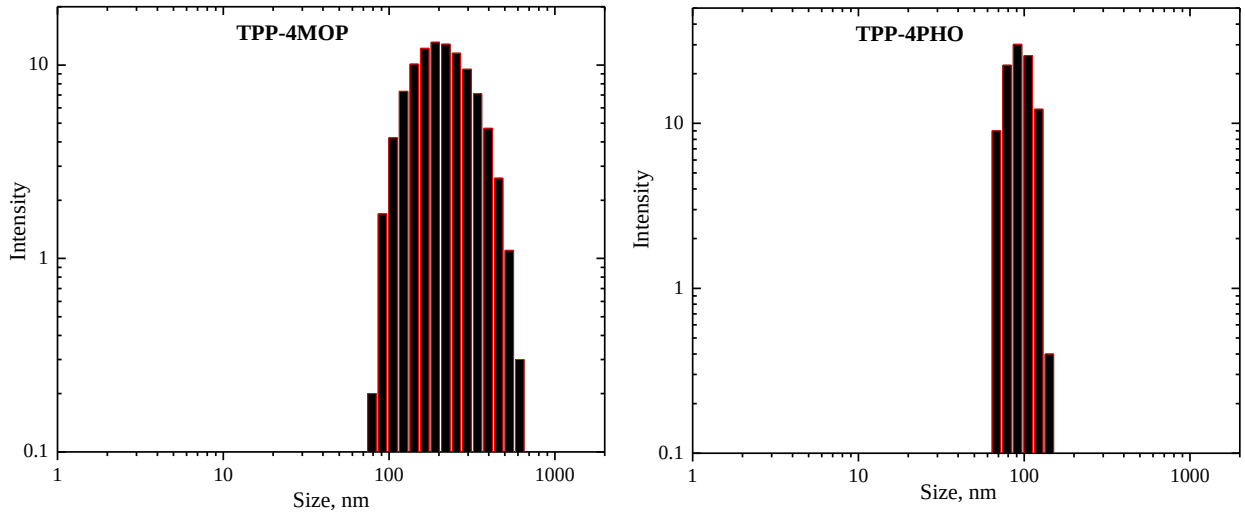

Figure S9 Size distribution of of nanoaggregates of TPP derivatives in THF-Water mixture of f_w = 90%, obtained by DLS measurements.

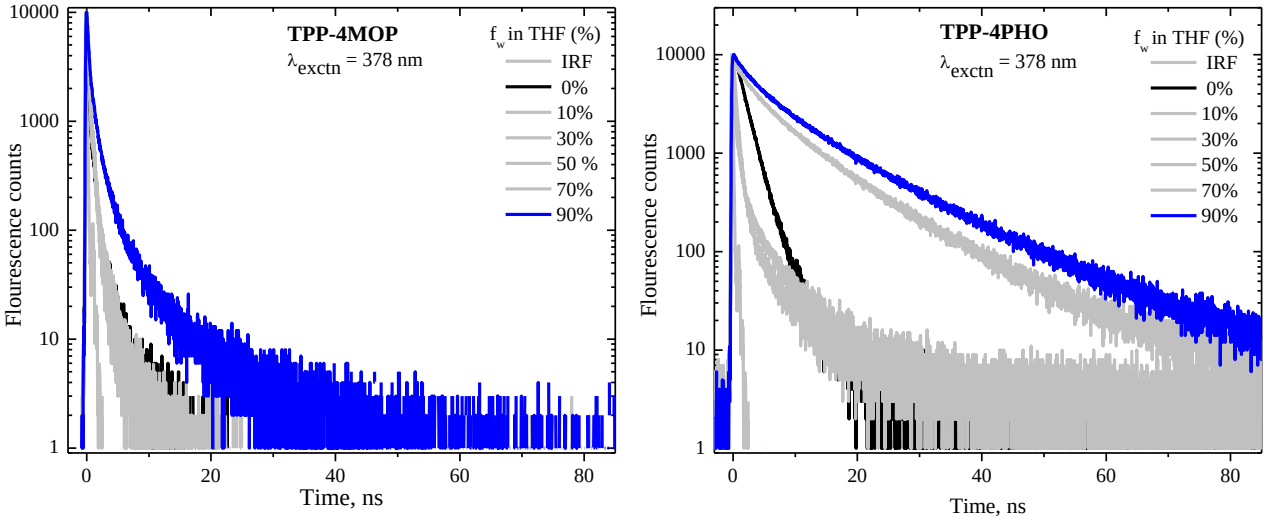

Figure S10 Fluorescent decay profile of TPP derivatives in THF with increase of f_w

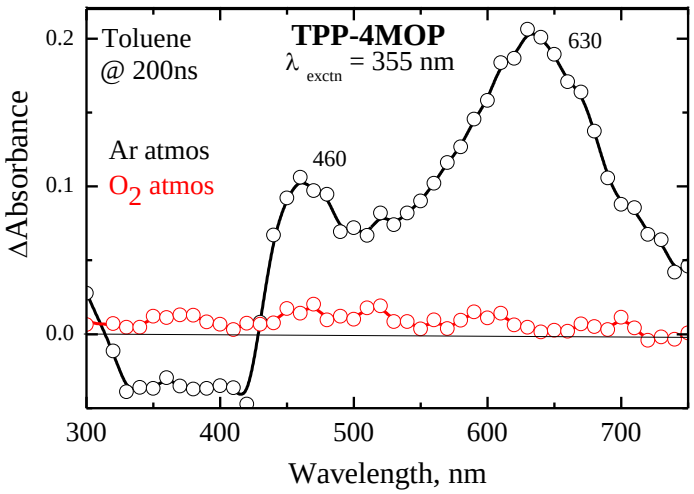

Figure S11 Nanosecond transient absorption spectra of **TPP-4MOP** at 200 ns obtained upon excitation at 355 nm in argon and oxygen saturated toluene.

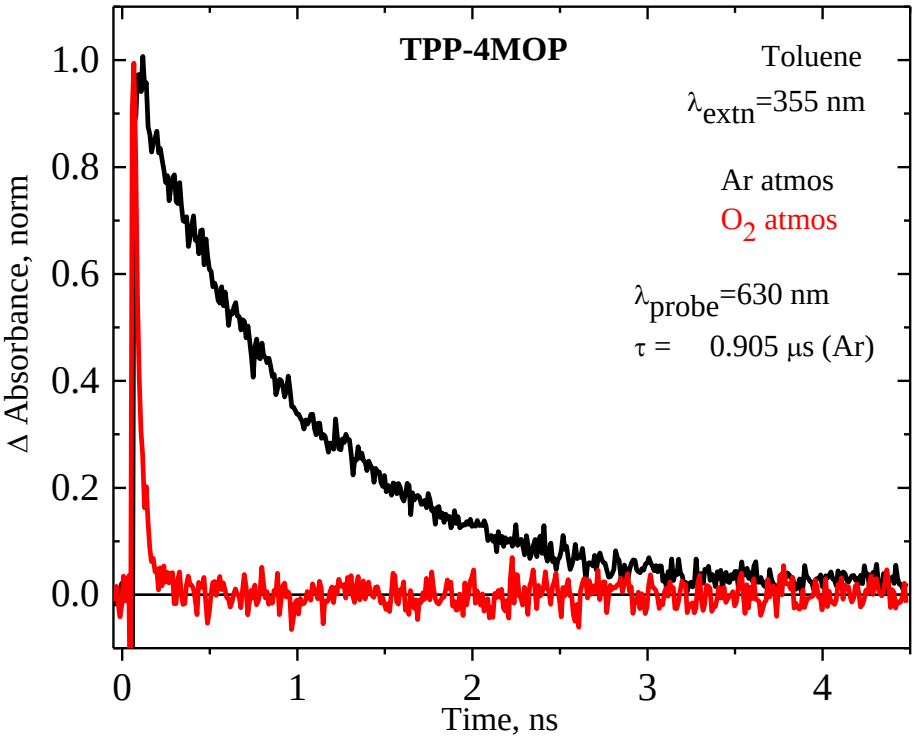

Figure S12 Kinetics probed at 630 nm for **TPP-4MOP** in argon and oxygen saturated toluene.

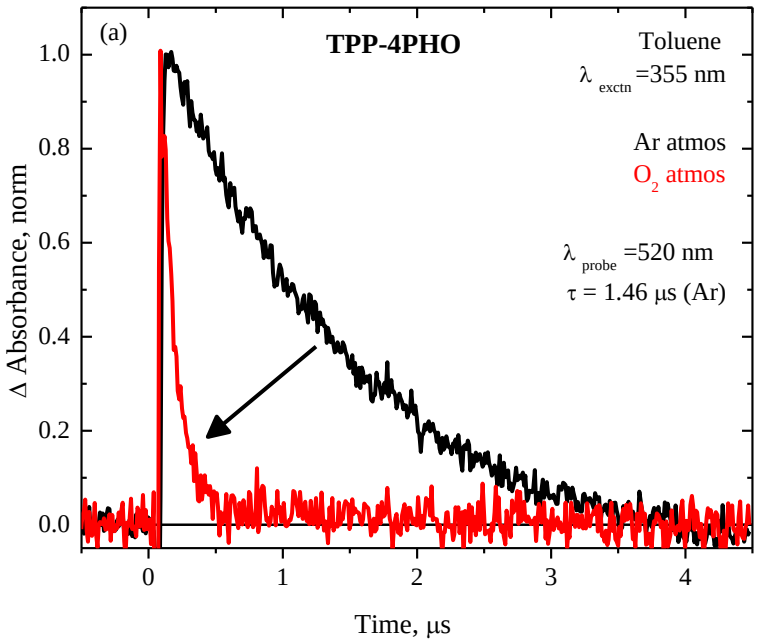

Figure S13 Kinetics probed at 520 nm for **TPP-4PHO** in argon and oxygen saturated toluene.

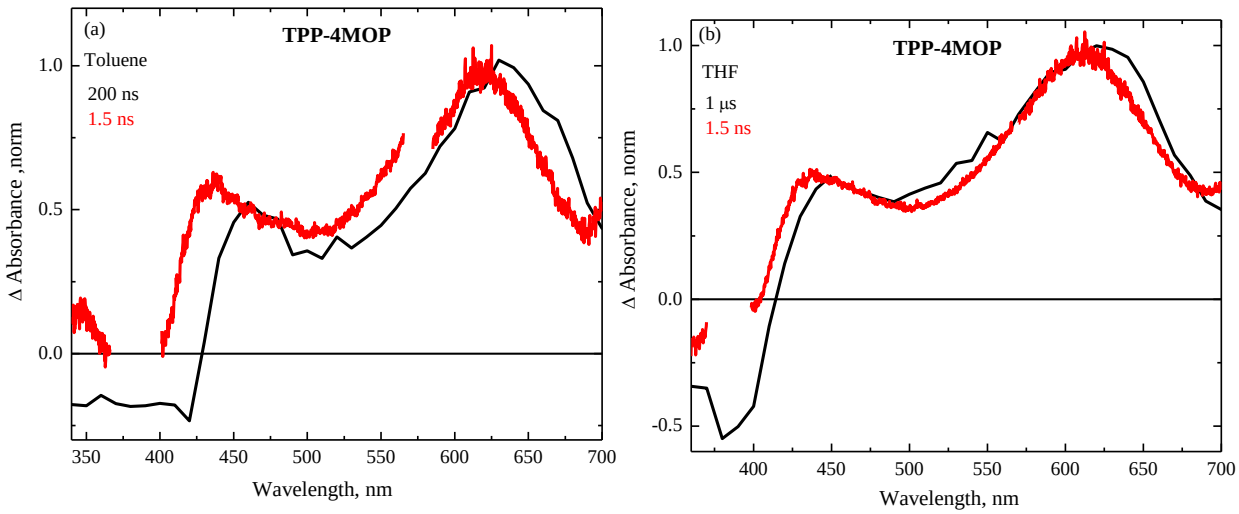

Figure S14 Nanosecond transient absorption spectra is overlayed with femtosecond transient spectra of **TPP-4MOP** in toluene (a) and THF (b) for comparison.

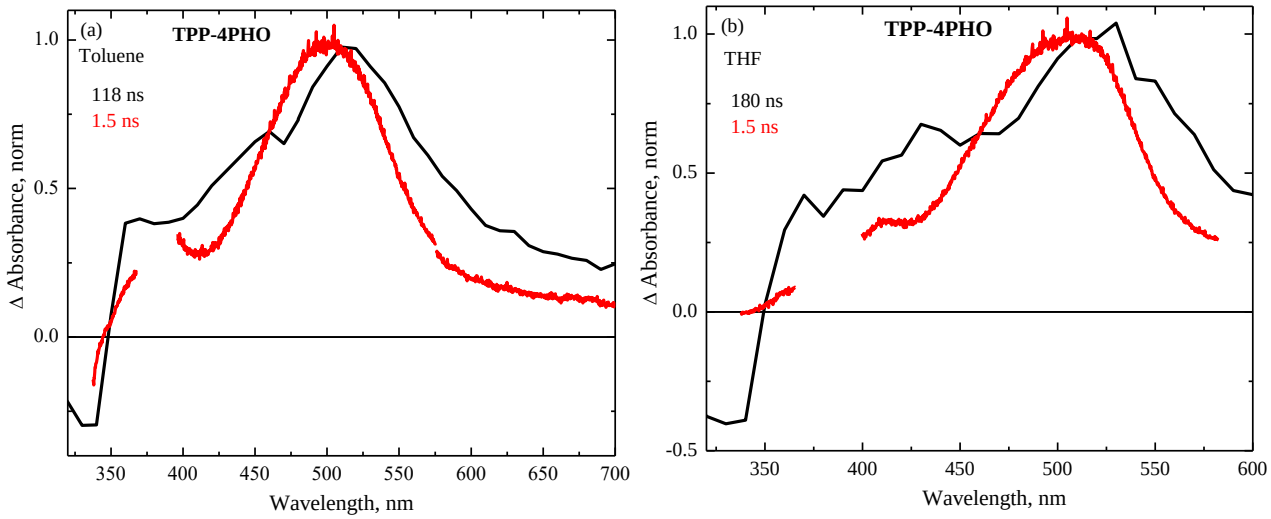

Figure S15 Nanosecond transient absorption spectra is overlayed with femtosecond transient spectra of **TPP-4PHO** in toluene (a) and THF (b) for comparison.

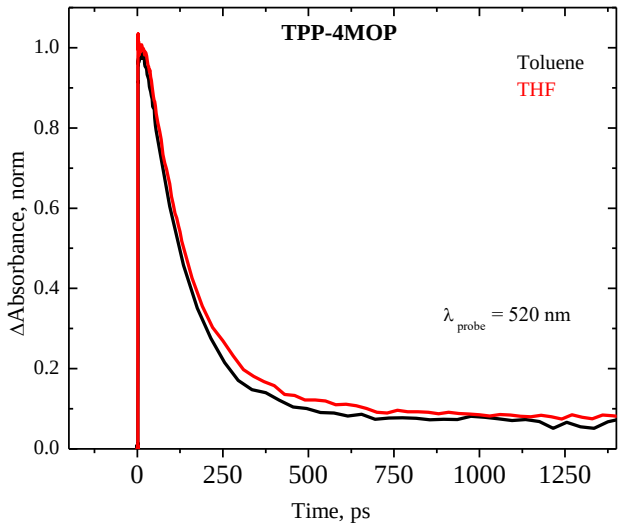

Figure S16 Femtosecond transient absorption decay of **TPP-4MOP** in toluene and THF upon excitation at 385 nm.

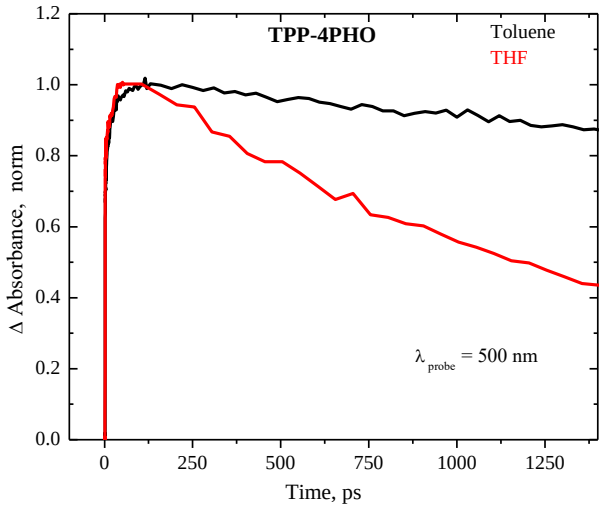

Figure S17 Femtosecond transient absorption decay of **TPP-4PHO** in toluene and THF upon excitation at 378 nm.

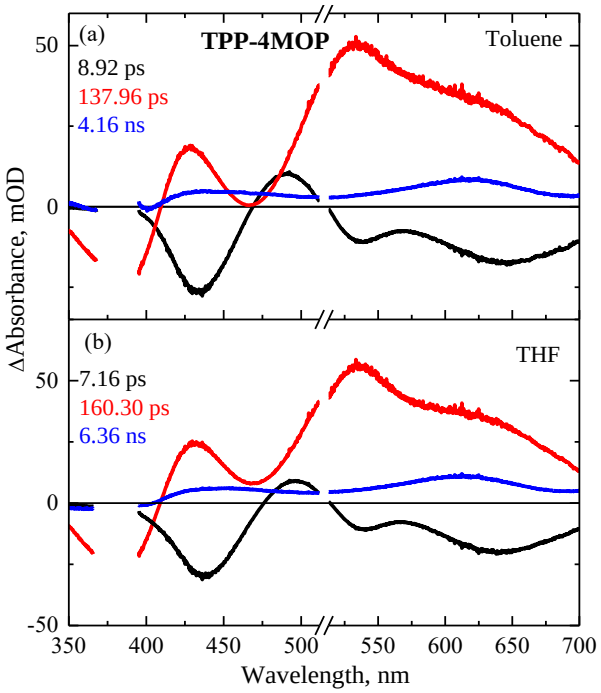

Figure S18 Decay associated differential spectra of **TPP-4MOP** in toluene (a) and THF (b).

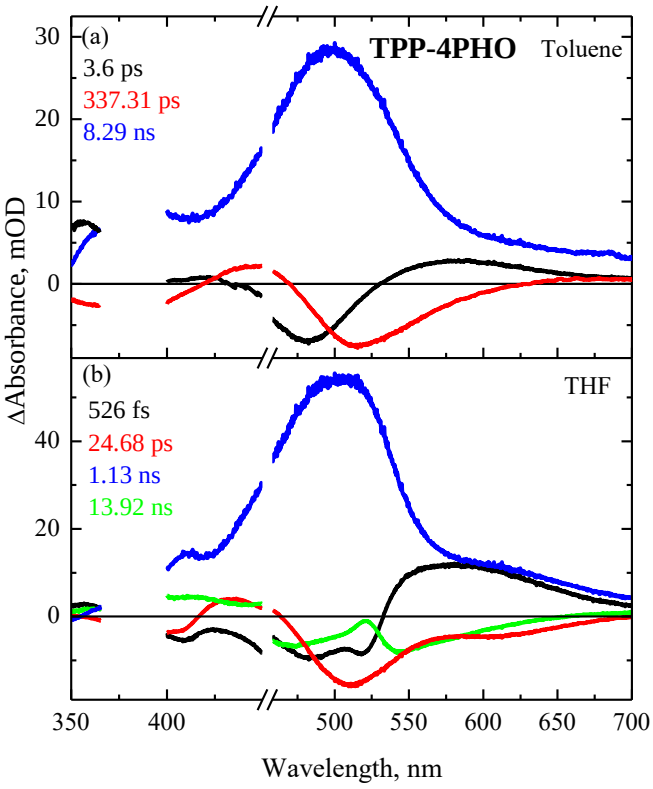

Figure S19 Decay associated differential spectra of **TPP-4PHO** in toluene (a) and THF (b).

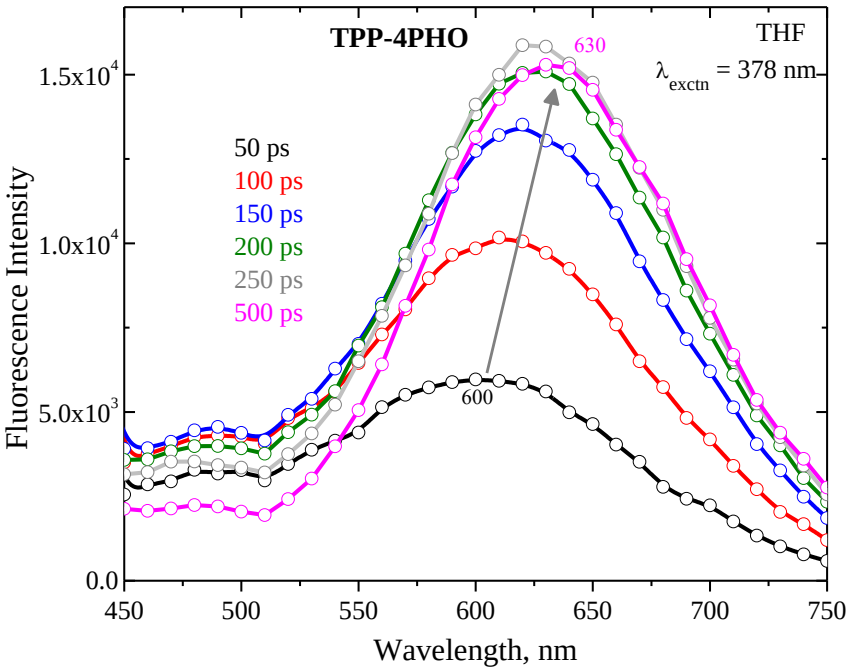

Figure S20 Time resolved emission spectra of **TPP-4PHO** in THF.

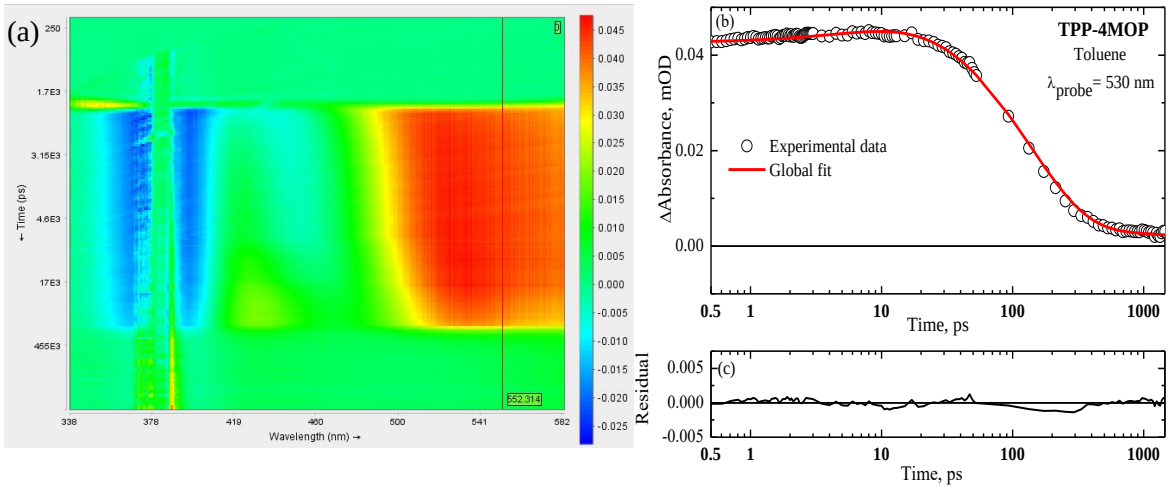

Figure S21 (a). Heat map of fsTAS of **TPP-4MOP** in toluene as a function of time delay (vertical) and probe wavelength (horizontal) in 1.47 ns time window upon excitation 385 nm. (b). The time profile at ESA maximum of 530 nm (open circle) along with three exponential fit (solid line) and residual (c) obtained from global analysis.

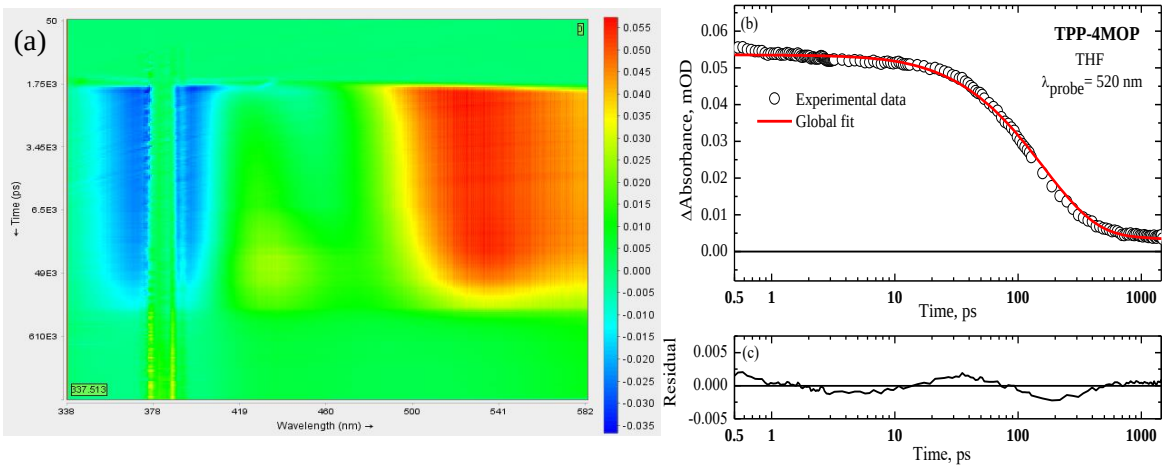

Figure S22 (a). Heat map of fsTAS of **TPP-4MOP** in THF as a function of time delay (vertical) and probe wavelength (horizontal) in 1.47 ns time window upon excitation 385 nm. (b). The time profile at ESA maximum of 520 nm (open circle) along with three exponential fit (solid line) and residual (c) obtained from global analysis.

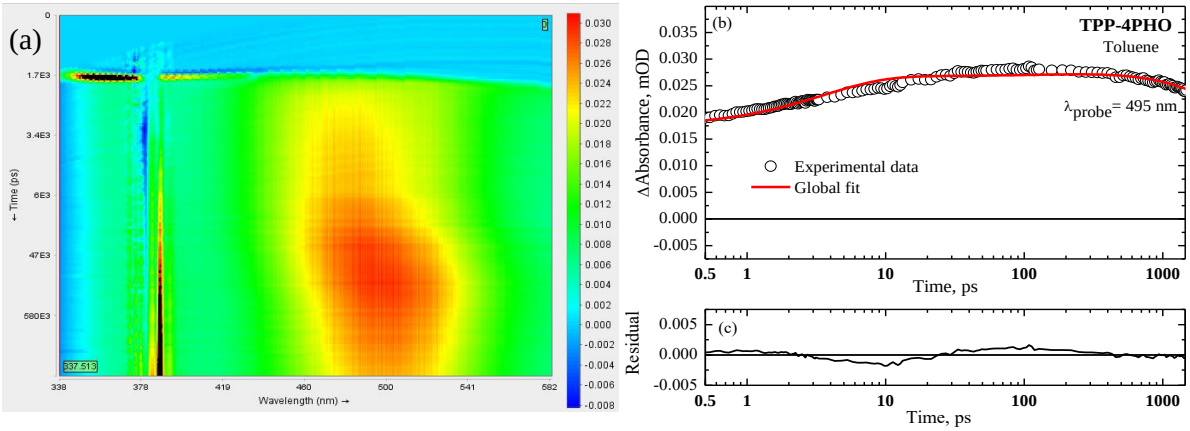

Figure S23 (a). Heat map of fsTAS of **TPP-4PHO** in toluene as a function of time delay (vertical) and probe wavelength (horizontal) in 1.47 ns time window upon excitation 385 nm. (b). The time profile at ESA maximum of 495 nm (open circle) along with three exponential fit (solid line) and residual (c) obtained from global analysis.

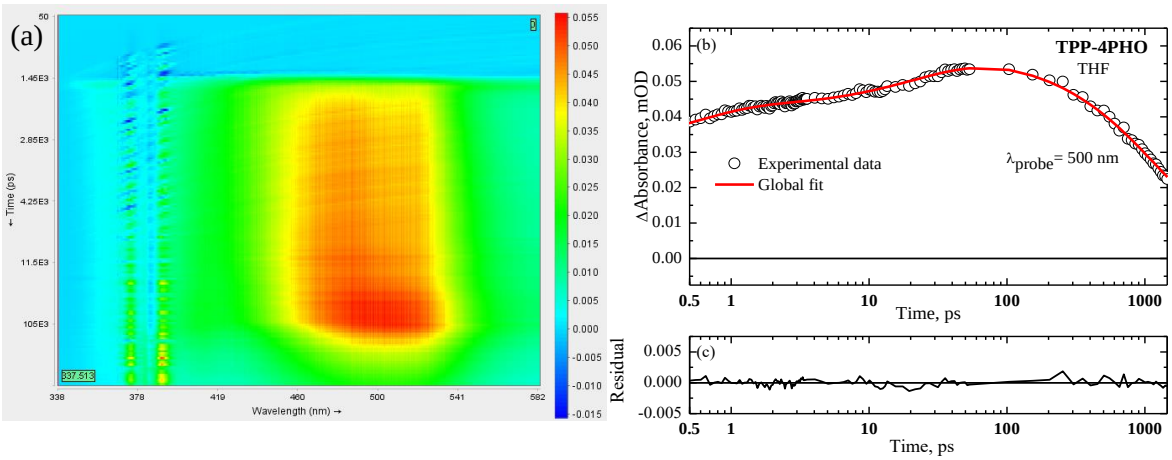

Figure S24 (a). Heat map of fsTAS of **TPP-4PHO** in THF as a function of time delay (vertical) and probe wavelength (horizontal) in 1.47 ns time window upon excitation 385 nm. (b). The time profile at ESA maximum of 500 nm (open circle) along with four exponential fit (solid line) and residual (c) obtained from global analysis.

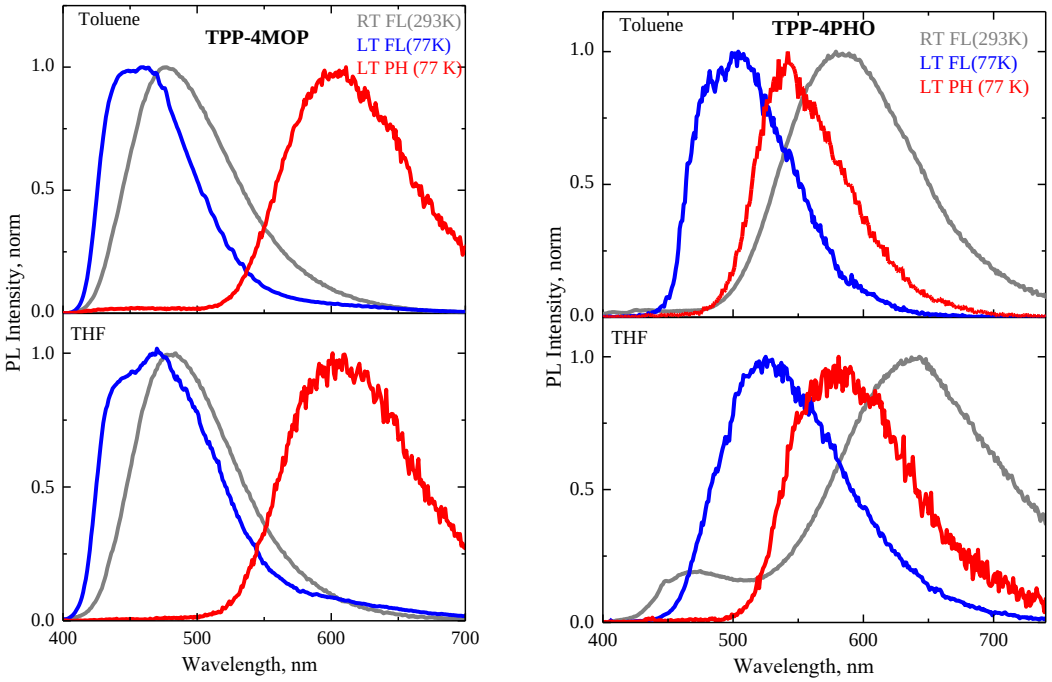

Figure S25 Room (grey) and low (77K) temperature fluorescence spectra (red) and low temperature phosphorescence spectra (red) of TPP derivatives in toluene and THF (λ_{exctn} =385 nm) in argon atmosphere.

Table S1 Electrochemical data of TPP derivatives.

	E_{ox}, V	E_{red}, V	HOMO[a], eV	LUMO[b], eV
TPP-4MOP	+0.34, +0.80	-1.25	-5.20	-3.15
TPP-4PHO	+0.38	-1.25	-4.78	-3.15
TPP	+0.35	-1.25	-4.75	-3.15

[a] Calculated by $E_{HOMO} = -(E_{ox} + 4.78 - E_{ox}(Fc))$. [b] Calculated by $E_{LUMO} = -(E_{red} + 4.78 - E_{ox}(Fc))$.Redox potentials of the compounds were determined with ferrocene (Fc) as the internal standard (0 V).

Table S2 Gibbs free energy change (ΔG_{CS}) of charge separation of TPP derivatives.

TPP Derivatives	Solvent	E_{00}[a], eV	ΔG_{CS}[b], eV
TPP-4MOP	Toluene	2.90	1.21
	THF	2.90	-0.98
TPP-4PHO	Toluene	2.65	0.12
	THF	2.65	-1.24

[a] Calculated from the cross point of normalized absorption and emission spectra at singlet excited state. Calculate using Rehm−Weller equation.

Table S3 Results of CAM-B3LYP/6-31G(d) calculations for TPP derivatives in gaseous medium.

Compound	λ_{max} (nm)[a]	f_{os}[b]	Major Transitions (weight)	μ_g[c],D	μ_e[d],D	E_{S1vert} (eV)	E_{T1vert} (eV)	$E_{HOMO-LUMO}$ (eV)	ΔE_{ST}
TPP-4MOP	271.22	1.07	HOMO-2→LUMO (100%)	0.23	0.33	3.71	1.85	5.87	1.86
	330.40	0.77	HOMO→LUMO+1 (100%)						
	334.08	0.69	HOMO→LUMO (100%)						
TPP-4PHO	362.8	0.102	HOMO → LUMO (50.59%) HOMO-1 → LUMO+1 (20.70%) HOMO → LUMO+2 (16.48%) HOMO-2 → LUMO+2 (12.23%)	0.24	9.90	3.41	2.00	5.00	1.41
	360.32	0.571	HOMO-1 → LUMO (49.10%) HOMO → LUMO+1 (23.35%) HOMO-1 → LUMO+2 (18.62%) HOMO-3 → LUMO (8.93%)						

359.38	0.040	HOMO → LUMO (43.74%) HOMO → LUMO+2 (31.47%) HOMO-1 → LUMO+1 (24.79%)
311.8	0.280	HOMO-4 → LUMO+1 (37.78%) HOMO-2 → LUMO+1 (26.54%) HOMO-3 → LUMO (19.88%) HOMO-1 → LUMO (15.80%)
303.44	0.314	HOMO-4 → LUMO (45.82%) HOMO-1 → LUMO+1 (27.86%) HOMO-3 → LUMO+1 (26.32%)
290	0.244	HOMO-4 → LUMO+1 (63.64%) HOMO → LUMO+1 (36.36%)
282.86	0.110	HOMO-19 → LUMO+1 (30.60%) HOMO → LUMO+3 (19.96%) HOMO-1 → LUMO+6 (11.57%) HOMO → LUMO+15 (10.89%) HOMO-1 → LUMO+11 (9.66%)
262.15	0.102	HOMO → LUMO+15 (54.74%) HOMO-1 → LUMO+9 (15.68%) HOMO-1 → LUMO+20 (14.89%) HOMO → LUMO+4 (14.69%)

[a]λ_{max} value obtained from the simulated absorption spectrum. [b]Oscillatory strength. [c]ground state dipole moment.[d] excited state dipole moment.

Table S4 Singlet energy and triplet energy of TPP derivatives in different solvents.

TPP Derivatives	Solvent	E_{S1}[a], eV	E_{S1}[b], eV	E_{T1}[c], eV	ΔE_{ST} [d], eV
	Toluene	2.95	3.00	2.38	0.62
TPP-4MOP	**THF**	2.95	3.00	2.33	0.67
	Toluene	2.55	2.74	2.52	0.22
TPP-4PHO	**THF**	2.47	2.70	2.42	0.28

[a] measured from onset of room temperature fluorescence, [b] measured from onset of low temperature (77 K) fluorescence, [c] measured from onset of phosphorescence spectra at low temperature (77K), [d] Singlet-triplet energy gap, $\Delta E_{ST} = E_{S1}{}^{b} - E_{T1}{}^{c}$

References

1. Frisch, M. J.; Trucks, G. W.; Schlegel, H. B.; Scuseria, G. E.; Robb, M. A.; Cheeseman, J. R.; Scalmani, G.; Barone, V.; Petersson, G. A.; Nakatsuji, H.; Li, X.; Caricato, M.; Marenich, A. V.; Bloino, J.; Janesko, B. G.; Gomperts, R.; Mennucci, B.; Hratchian, H. P.; Ortiz, J. V.; Izmaylov, A. F.; Sonnenberg, J. L.; Williams; Ding, F.; Lipparini, F.; Egidi, F.; Goings, J.; Peng, B.; Petrone, A.; Henderson, T.; Ranasinghe, D.; Zakrzewski, V. G.; Gao, J.; Rega, N.; Zheng, G.; Liang, W.; Hada, M.; Ehara, M.; Toyota, K.; Fukuda, R.; Hasegawa, J.; Ishida, M.; Nakajima, T.; Honda, Y.; Kitao, O.; Nakai, H.; Vreven, T.; Throssell, K.; Montgomery Jr., J. A.; Peralta, J. E.; Ogliaro, F.; Bearpark, M. J.; Heyd, J. J.; Brothers, E. N.; Kudin, K. N.; Staroverov, V. N.; Keith, T. A.; Kobayashi, R.; Normand, J.; Raghavachari, K.; Rendell, A. P.; Burant, J. C.; Iyengar, S. S.; Tomasi, J.; Cossi, M.; Millam, J. M.; Klene, M.; Adamo, C.; Cammi, R.; Ochterski, J. W.; Martin, R. L.; Morokuma, K.; Farkas, O.; Foresman, J. B.; Fox, D. J. *Gaussian 16 Rev. C.01*, Wallingford, CT, 2016.
2. Adarsh, N.; Avirah, R. R.; Ramaiah, D., Tuning Photosensitized Singlet Oxygen Generation Efficiency of Novel Aza-BODIPY Dyes. *Org. Lett.* **2010,** *12* (24), 5720-5723.
3. Topchiy, M. A.; Asachenko, A. F.; Nechaev, M. S., Solvent-Free Buchwald–Hartwig Reaction of Aryl and Heteroaryl Halides with Secondary Amines. *Eur. J. Org. Chem.* **2014,** (16), 3319-3322.